ARTICLES

Dissociative Photoionization of $Mo(CO)_6$ in the Photon Energy Range of 8−40 eV

Fei Qi[†] and Shihe Yang*

Department of Chemistry, Hong Kong University of Science & Technology, Clear Water Bay, Kowloon, Hong Kong

Liusi Sheng, Weiquan Ye, Hui Gao, and Yunwu Zhang

National Synchrotron Radiation Laboratory, University of Science & Technology of China, Hefei, Anhui 230026, China

Shuqin Yu

Department of Chemical Physics, University of Science & Technology of China, Hefei, Anhui 230026, China

Received: March 10, 1997; In Final Form: July 3, 1997[⊗]

Twelve ions have been observed in the dissociative photoionization studies of $Mo(CO)_6$ using a synchrotron radiation source in the photon energy range of 8−40 eV. The photoionization efficiency (PIE) curves of these ions from the dissociative ionization of $Mo(CO)_6$ have been measured for the first time. Appearance potentials (AP) of all the ions have been determined from their PIE curves and these AP values, in turn, bring about a series of bond dissociation energy (BDE) data for the intermediate ions produced by photoionization/fragmentation.

I. Introduction

Among the group VIB transition metal hexacarbonyls, $Cr(CO)_6$ is the most studied compound concerning the thermochemistry of its ionic fragments.[1,2] The bond dissociation energies (BDE) of $CO-Cr(CO)_n^+$ have been estimated by electron impact ionization[3,4] and photoionization.[5] The observed reduction in BDE of $CO-Cr(CO)_n^+$ compared to that of $CO-Cr(CO)_n$ revealed the importance of the π^* back-donation from the metal to the ligands in the bonding of the metal carbonyl compound.

Similar measurements on $Mo(CO)_6^+$ have been rather limited. Most fragmentation studies on $Mo(CO)_6^+$ to date used the electron impact ionization method.[3,4] Winters and Kiser have observed $Mo(CO)_n^+$ ($n = 0-6$), doubly charged ions $Mo(CO)_n^{2+}$ ($n = 1-3$), and the carbide ion MoC^+ from $Mo(CO)_6$ using 70 eV electron impact ionization.[3] Michels and coworkers observed only seven ions $Mo(CO)_n^+$ ($n = 0-6$) produced with a 50 eV electron beam.[4] Both groups have estimated the appearance potentials (AP) of the observed fragment ions. Although multiphoton ionization/fragmentation of $Mo(CO)_6$ in the UV and visible regions has been under scrutiny,[6] no single-photon ionization study of $Mo(CO)_6$ has been reported. Since it is generally accepted that thermochemistry data measured by photoionization is more accurate than that measured by electron impact ionization, it is desirable to derive the thermochemical data of the ionic fragments of $Mo(CO)_6$ by studying the fragmentation of $Mo(CO)_6^+$ generated by single-photon ionization. Photoionization, especially when armed with the widely tunable and powerful synchrotron radiation source from UV to extreme UV is a valuable technique for thermochemical measurements concerning the ion fragmentation and its dynamics.

Photoelectron−photoion coincidence (PEPICO) technique has proven to be a powerful technique for studying ion fragmentation dynamics.[5,7,8] By the combination of this technique with the synchrotron radiation source with a wide range of photon energies from UV to the extreme ultraviolet region, energetics and fragmentation dynamics of intermediate ions, produced by photoionization of the parent molecule followed by dissociation, can be studied. Recently, we have studied $Cr(CO)_6$ by applying a varied version of this technique.[9] By detecting all the photoelectrons from photoionization without energy selection, we obtained the photoionization efficiency (PIE) curves of all the observed ions from the dissociative photoionization of $Cr(CO)_6$. In this study, aside from sequential fragmentation of the parent ion, metal carbide and doubly charged ions from $Cr(CO)_6$ were identified.

In the present work, we focus on the fragmentation of $Mo(CO)_6^+$ produced by the photoionization of $Mo(CO)_6$ using the synchrotron radiation in the photon energy range of 8−40 eV. We report the PIE curves of all the ions resulting from the dissociative photoionization of $Mo(CO)_6$ and derive from these PIE data the thermodynamic information concerning the ion fragmentation processes.

II. Experimental Section

Details of the experimental set up can be found in previous publications.[10,11] Synchrotron radiation from the 800 MeV electron storage ring (National Synchrotron Radiation Laboratory, Hefei, China) was monochromized by using a 1 m Seya-Namioka monochromator equipped with three gratings (2400, 1200, and 600 lines/mm) covering the wavelength range ~300−

* To whom correspondence should be addressed.
[†] On leave from National Synchrotron Radiation Laboratory, Hefei, China.
[⊗] Abstract published in *Advance ACS Abstracts,* September 1, 1997.

S1089-5639(97)00884-0 CCC: $14.00

6000 Å. The gratings of 2400 and 1200 lines/mm are coated with Au and Ir, and blazed at around 550 and 1400 Å, respectively. The wavelength of the monochromator was carefully calibrated with the known ionization potentials and autoionization peaks of the inert gases Ne and Ar. The wavelength resolution is about 1.5 Å with 200 μm entrance and exit slits. The photon flux was monitored by a sodium salicylate coated glass window with a PMT behind the ionization chamber. PIE curves were normalized by the photon flux. In the wavelength region longer than the LiF cutoff (1050 Å), a LiF window (1 mm thick) was used to eliminate higher order radiation of the dispersed light.

A time-of-flight (TOF) mass spectrometer was employed for the VUV photoionization/fragmentaion studies. Photoelectrons and photoions produced by the VUV light were drawn out of the photoionization region in opposite directions and detected separately by a channeltron electron multiplier and an MCP detector. The electron flight time from the photoionization region to the electron detector is ≤ 0.1 μs and can thus be ignored compared to the ion flight time. Mass analysis was achieved by TOF mass spectrometry which uses the photoelectron pulse (in our PIE studies, this pulse includes both threshold and nonthreshold photoelectrons) to start and the photoion pulse to stop a time-to-amplitude converter (TAC). The output of the TAC was sorted in a MCA. A mass spectrum was obtained as the total number of coincidence vs the flight time of the ions. The TOF tube is 1000 mm long and its mass resolution is typically ~120. A specified ion can be monitored by selecting the TAC amplitude, and the TAC output is then sent to a counter through a single-channel analyzer (SCA). The ion signal intensity was carefully controlled so as to avoid the parasitic effect in using the TAC for the TOF measurements. The parent and daughter ions $Mo(CO)_n^+$ ($n = 0-6$) were simultaneously tracked through the TAC/SCA as the wavelength was scanned with a wavelength increment of 1 Å, yielding PIE curves of these ions. Owing to the weaker signals of $Mo(CO)_n^{2+}$ ($n = 1-3$) and MoC^+, these ions were not selected for the wavelength scanning. Their PIE curves were obtained by recording a series of time-of-flight mass spectra at different wavelengths. The APs of $Mo(CO)_n^{2+}$ ($n = 1-3$) and MoC^+ were estimated based on the series of mass spectra and taken as the wavelength at which the ion disappears.

$Mo(CO)_6$ was obtained from Strem Chemicals with a stated purity of 99% and used without further purification. In this experiment, the vapor of $Mo(CO)_6$ was introduced by a 1.5 mm diameter hole and was carried by He (~400 Torr), forming a continuous beam through a 70 μm diameter nozzle downstream. The molecular beam travels from the source chamber into the ionization chamber through a 1.5 mm skimmer. The pressure of the ionization chamber was $\sim 5 \times 10^{-6}$ Torr when the molecular beam was introduced. No cluster was observed under this condition, so no fragment ions were considered to originate from cluster dissociation.

III. Results

Typical TOF mass spectra at different photon energies are given in Figure 1. As can be seen from the figure, in addition to the parent ion and the CO-elimination fragments $Mo(CO)_6^+$ ($n = 0-6$), other fragments, including the carbides MoC^+ and $MoC(CO)^+$ and the doubly charged species $Mo(CO)_n^{2+}$ ($n = 1-3$) can be identified. These species were observed previously in the electron impact ionization mass spectra of $Mo(CO)_6$.[3] Figure 1 also shows that, as the photon energy increases, $Mo(CO)_n^+$ ($n = 4-6$) gradually decreases. $Mo(CO)_5^+$ disappears at higher photon energy, but $Mo(CO)_n^+$ ($n = 0-3$) gain intensity

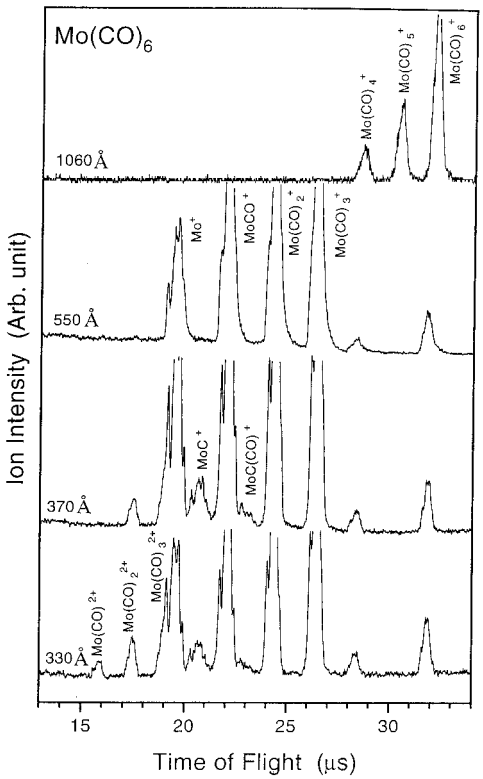

Figure 1. Typical dissociative photoionization TOF mass spectra at different photon energies.

at the same time. Above 1050 Å, $Mo(CO)_n^+$ ($n = 4-6$) are the only fragments which can be observed in the mass spectra. However, at all the photon energies we investigated, the parent ion always appeared; its intensity decreased only slightly with the increasing photon energy.

The PIE curves of the parent ion $Mo(CO)_6^+$ and of all the CO-elimination fragment ions $Mo(CO)_5^+$, $Mo(CO)_4^+$, $Mo(CO)_3^+$, $Mo(CO)_2^+$, $MoCO^+$, and Mo^+ are presented in Figures 2−4, respectively. The AP in each PIE curve has been determined by the linear extrapolation method.[10−12] In our data treatment, we ignored the thermal energy distribution of the parent molecule. Under the nozzle expansion condition described above, certain extent of cooling is expected (below 200 K). The thermal energy has the effect of lowering the observed APs. In addition, no correction has been made for possible reverse activation barriers and kinetic shifts in determining the APs. As these factors tend to shift the observed onset to higher energies, the APs we estimated only give upper limits. Similar data analysis has been carried out by other researchers and appears to be useful for studying ion fragmentation processes.[7,10−14]

Since the ion signals of the carbide fragments and the doubly charged species are quite weak, continuous wavelength scanning of these fragment channels was not pursued. Instead, we took the TOF mass spectra with 5 Å intervals from 300 to 460 Å and constructed PIE curves based on the mass spectra. Shown in Figure 5 are the PIE curves of $Mo(CO)^{2+}$, $Mo(CO)_2^{2+}$, $Mo(CO)_3^{2+}$, and MoC^+, constructed from the TOF mass spectra. The Aps of these ion fragments were determined as the photon energy at which the ion disappears. We did not attempt to construct the PIE curve of $MoC(CO)^+$ due to its weaker ion intensity, but the AP of $MoC(CO)^+$ can be estimated to be around 23.39 eV.

Figure 6 plots the relative ion abundance as a function of photon energy for the parent ion and the CO-elimination fragment ions from $Mo(CO)_6$. The ion intensities are normal-

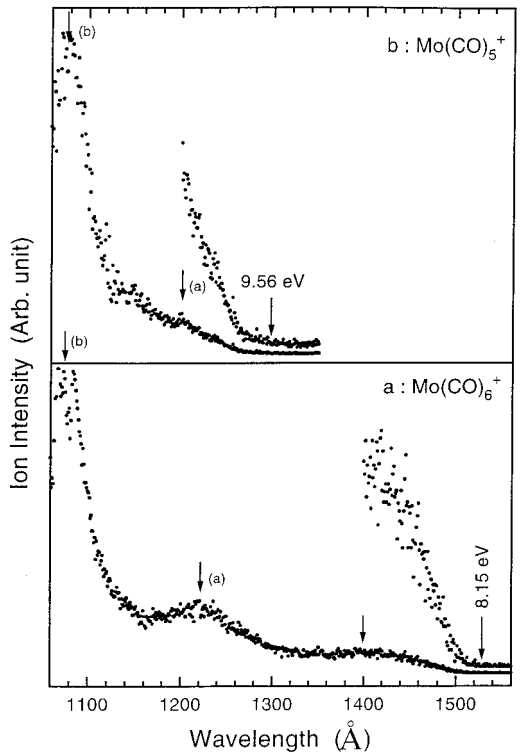

Figure 2. Photoionization efficiency curves of (a) $Mo(CO)_6^+$, and (b) $Mo(CO)_5^+$ from $MO(CO)_6$.

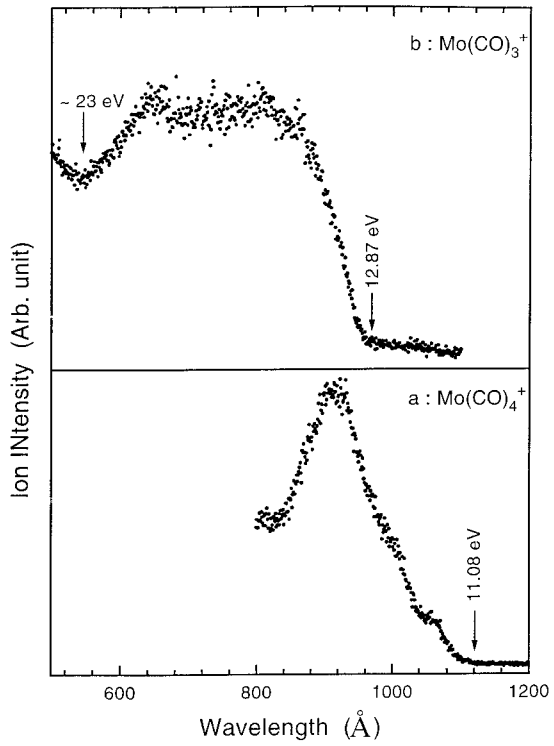

Figure 3. Photoionization efficiency curves of (a) $Mo(CO)_4^+$, and (b) $Mo(CO)_3^+$ from $Mo(CO)_6$.

ized so that their intensity sum is 100 at any wavelength. At low energy, the parent molecule ion predominates. As the photon energy is increased the fragment ions "grow in" in order of their increasing APs, e.g., $Mo(CO)_5^+$, $Mo(CO)_4^+$, etc. Subsequently, the abundance of each of these ions passes through a maximum (except for Mo^+) and then decreases to a nearly constant value at higher energy. Overall, the relative ion abundance graph is quite similar to those obtained from electron impact ionization.[3] Since the relative ion abundance

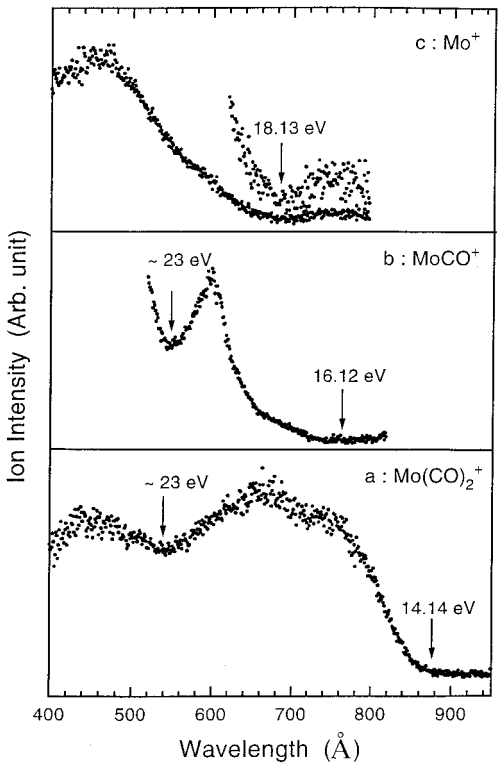

Figure 4. Photoionization efficiency curves of (a) $Mo(CO)_2^+$, (b) $MoCO^+$, and (c) Mo^+ from $Mo(CO)_6$.

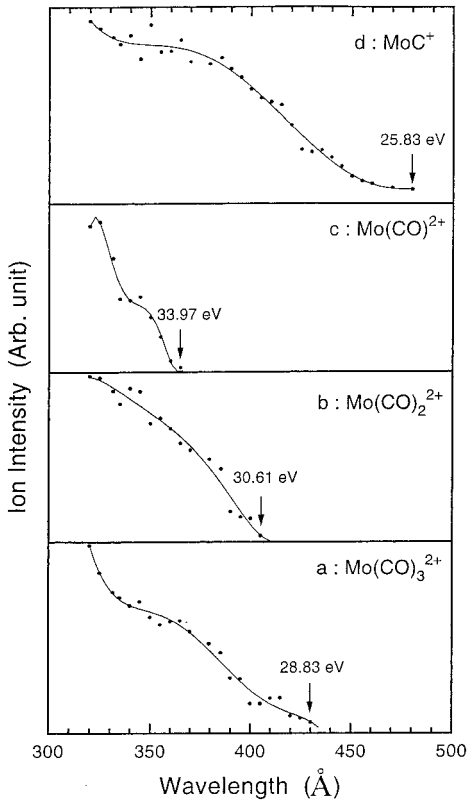

Figure 5. Photoionization efficiency curves of (a) $Mo(CO)_3^{2+}$, (b) $Mo(CO)_2^{2+}$, and (c) $Mo(CO)^{2+}$ and (d) MoC^+ from $Mo(CO)_6$.

graph is constructed from a series of TOF mass spectra with a relatively large wavelength intervals (5−10 Å), some fine features are not as clear as those observed in the corresponding PIE curves obtained by the continuous wavelength scanning method.

In Figure 7 the He I photoelectron spectrum (PES) of $Mo(CO)_6$ reported previously is reproduced.[15] It is interesting to

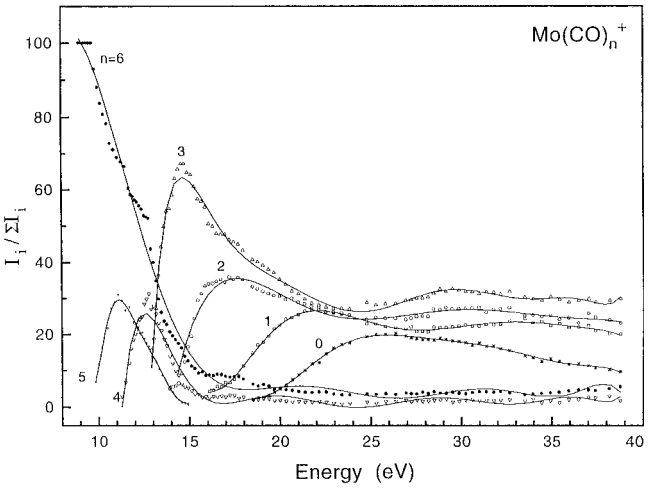

Figure 6. Relative intensities of the parent and fragment ions from $Mo(CO)_6$ as a function of photon energy. The intensity sum of all the observed ions is set to be 100 at all the wavelengths in the plot.

compare the PES of $Mo(CO)_6$ with the onsets of the ion fragments from $Mo(CO)_6$. The first peak centered at around 8.4 eV arises from the ejection of an electron from the $2t_{2g}$ orbital with mainly the Mo(4d) character. The PE peak observed at ionization energy ~13.4 eV was assigned to an electronic states corresponding to the removal of an electron from the $8t_{1u}$ orbital.[9,16,17] The PE peaks in the energy range of 14−16 eV and around 17.6 eV correspond to the removal of electrons from the 5σ and 1π and 4σ orbitals of the CO ligands, respectively.[9,16,17] The energy thresholds for the formation of $Mo(CO)_n^+$ ($n = 0-6$) are indicated in Figure 7. The thresholds for the formation of $Mo(CO)_n^+$ ($n = 0-3$) approximately coincide with the $8t_{1u}$, 5σ and 1π, and 4σ PE peaks, respectively. The onsets for the elimination of the first two CO ligands from $Mo(CO)_6$ occur in the valley region of the photoelectron spectrum. Most likely, these fragments are produced from the vibrational autoionization of $Mo(CO)_6$ as suggested for $Cr(CO)_6$ by Das et al.[5]

IV. Discussion

The APs derived from Figures 2−5 are tabulated in Table 1 along with the values measured by other researchers. The error bars are also listed. These error bars only reflect either the band width of our monochromator or the wavelength interval of the data points for performing the measurements. It appears through a rough comparison that the data of Winters et al.[3] and Foffani et al.[18] are close to our result at lower energy, whereas the data of Michels and co-workers agree with our result at higher energy.[4] The ionization potential (IP) of $Mo(CO)_6$ we obtained is lower than all the reported values using electron impact ionization and photoelectron spectroscopy in literature.[3,4,19−21] The IP of $Mo(CO)_6$ was also measured by the photoionization method previously.[22] The IP value of 8.12 eV measured by Vileso and Kurbatov using photoionization[22b] is in good agreement with our result. It should be mentioned that, in measuring the APs of $Mo(CO)_n^+$ ($n = 5, 6$), we used a LiF filter which effectively eliminated the effect of higher order radiation from the grating. For the AP measurements of $Mo(CO)_n^+$ ($n = 0-4$), the grating of 2400 lines/mm was used without adding filter. According to our past experience, the effect of the second order radiation from this grating is negligible.[10] Due to the adoption of the continuous wavelength scanning procedure and the use of LiF fliter to cut off higher order radiation, the photoionization onset of the $Mo(CO)_6^+$ ion shown in Figure 2a is very clear. We therefore believe that the IP of $Mo(CO)_6$ we measured is reasonably accurate.

Some features in the PIE curves shown in Figures 2−4 can be clearly recognized. In the PIE curves of $Mo(CO)_6^+$ and $Mo(CO)_5^+$ shown in Figure 2, two pronounced features labeled a and b are noteworthy, which peak at around 10.2 and 11.5 eV, respectively. For $Mo(CO)_6^+$, there is one more peak at a longer wavelength (~1400 Å). It is interesting to compare this result to the total photoabsorption and photoionization cross sections of $Mo(CO)_6$ we measured previously.[23] The most pronounced peak b in the PIE curves of $Mo(CO)_6^+$ and $Mo(CO)_5^+$ matches closely to a sharp peak in the photoabsorption spectrum of $Mo(CO)_6$ and a bump in the photoionization spectrum of $Mo(CO)_6$ at the same wavelength. As pointed out previously, this peak corresponds to the excitation of one of the molecular orbitals localized on the CO ligands (5σ or 1π) to an unoccupied orbital, e.g., 2π (π^*). Similarly, peak a and the peak at ~1400 Å in the PIE curve of $Mo(CO)_6^+$ can also be related to the photoabsorption spectrum and photoionization spectrum of $Mo(CO)_6$.[23]

A valley is apparent in the PIE curves of $Mo(CO)_3^+$, $Mo(CO)_2^+$, and $MoCO^+$ shown in Figures 3b, 4a, and 4b respectively. These valleys can also be observed in the PIE curves of $Cr(CO)_2^+$ and $Cr(CO)^+$ from $Cr(CO)_6$.[9] Close examination of the PIE curves of $Mo(CO)_3^+$, $Mo(CO)_2^+$, and $MoCO^+$ in Figures 3b and 4a,b shows that the valleys are located at similar photon energies around 23 eV. The PIE curves of $Mo(CO)_n^+$ ($n \geq 4$) have not been extended to these photon energies, and we therefore do not know whether these valleys persist. The coincidence of the valleys in the PIE curves of $Mo(CO)_n^+$ ($n = 1-3$) suggests that these steps may have the same origin. Since no obvious dip was observed in the total photoionization yield spectrum of $Mo(CO)_6$,[23] we suspect that the parent ion $Mo(CO)_6^+$ may have preferentially survived at the photon energies (~23 eV), leading to a lower probability of forming the smaller fragment ions. Valleys at similar photon energies were observed in the PIE curves of $Cr(CO)_2^+$ and $Cr(CO)^+$ from $Cr(CO)_6$.[9]

From the AP values given in Table 1, the heats of formation of different ions produced from photoionization/fragmentation of $Mo(CO)_6$ can be estimated by the following equations:

$$\Delta H_{f\,298}^0(Mo(CO)_{6-m}^{x+}) = AP(Mo(CO)_{6-m}^{x+}) + \Delta H_{f\,298}^0(Mo(CO)_6) - m\Delta H_{f\,298}^0(CO) \quad (1)$$

$$\Delta H_{f\,298}^0(MoC(CO)_{5-m}^{+}) = AP(MoC(CO)_{5-m}^{+}) + \Delta H_{f\,298}^0(Mo(CO)_6) - (m-1)\Delta H_{f\,298}^0(CO) - \Delta H_{f\,298}^0(CO_2) \quad (2)$$

where $\Delta H_f^0{}_{298}(Mo(CO)_6)$, $\Delta H_f^0{}_{298}(CO)$, and $\Delta H_f^0{}_{298}(CO_2)$ are −218.5,[24] −26.41,[25] and −94.05 kcal/mol,[25] respectively, taken from literature. The derived heats of formation of the ions are also listed in Table 1 together with the literature values. A cursory inspection of the Table 1 shows that our results are roughly consistent in trend with those obtained by other groups using the electron impact ionization method but different in terms of the exact values.

The BDEs($(CO)_mMo^+-CO$) were calculated from the AP values in Table 1 and listed in Table 2 along with some literature values. In general, the agreement of our calculated results with those of the electron impact ionization method other groups is not so good in terms of the exact values. Since the photoionization onsets of the ions are all quite clear, we believe that the apparent BDEs we obtained should be reasonably accurate; by "apparent" we mean that the kinetic energy shift and reverse barrier effect have been ignored. Of course, the true BDEs still

TABLE 1: APs and Heats of Formation of the Ions from $Mo(CO)_6$

	AP (eV)						$\Delta H_f^0{}_{298}$ (kcal/mol)			
ions	this work	ref 4	ref 3	ref 18	others	assumed process	this work	ref 4	ref 3	ref 18
$Mo(CO)_6^+$	8.15 ± 0.01	8.46	8.23	8.30	8.25,[a] 8.2,[b] 8.5,[c] 8.12,[d] 8.227[e]	$Mo(CO)_6$ → $Mo(CO)_6^+ + e$	−30.6 ± 0.25	−23.4	−29	−27.1
$Mo(CO)_5^+$	9.56 ± 0.01	10.02	9.80	9.64		→ $Mo(CO)_5^+ + CO + e$	28.2 ± 0.25	39	34	30.2
$Mo(CO)_4^+$	11.08 ± 0.02	11.61	11.9	11.28		→ $Mo(CO)_4^+ + 2CO + e$	89.8 ± 0.45	102	109	94.4
$Mo(CO)_3^+$	12.87 ± 0.02	13.29	13.7	12.36		→ $Mo(CO)_3^+ + 3CO + e$	157.5 ± 0.45	167	177	145.8
$Mo(CO)_2^+$	14.14 ± 0.02	14.86	15.6	13.90		→ $Mo(CO)_2^+ + 4CO + e$	213.2 ± 0.45	230	247	207.7
$Mo(CO)^+$	16.12 ± 0.03	16.52	18.1	15.8		→ $Mo(CO)^+ + 5CO + e$	285.0 ± 0.70	295	331	277.9
Mo^+	18.13 ± 0.05	18.24	20.7	18.3		→ $Mo^+ + 6CO + e$	358.0 ± 1.2	361	417	362.0
$MoC(CO)^+$	(23.39) ± 0.20					→ $MoC(CO)^+ + CO_2 + 3CO + e$	(494.2) ± 5.0			
						or → $MoC(CO)^+ + O + 4CO + e$	(426.5) ± 5.0			
MoC^+	25.83 ± 0.30	27.2				→ $MoX^+ + XO_2 + 4XO + e$	576.8 ± 7.0		608	
						or → $MoC^+ + O + 5CO + e$	509.2 ± 7.0			
$Mo(CO)_3^{2+}$	28.83 ± 0.35	29.1				→ $Mo(CO)_3^{2+} + 3CO + 2e$	525.5 ± 8.0		532	
$Mo(CO)_2^{2+}$	30.61 ± 0.40	30.8				→ $Mo(CO)_2^{2+} + 4CO + 2e$	593.0 ± 9.0		597	
$Mo(CO)^{2+}$	33.97 ± 0.45	34.5				→ $Mo(CO)^{2+} + 5CO + 2e$	696.9 ± 10.0		709	

[a] Reference 19. [b] Reference 20. [c] Reference 21. [d] Reference 22b. [e] Reference 22a.

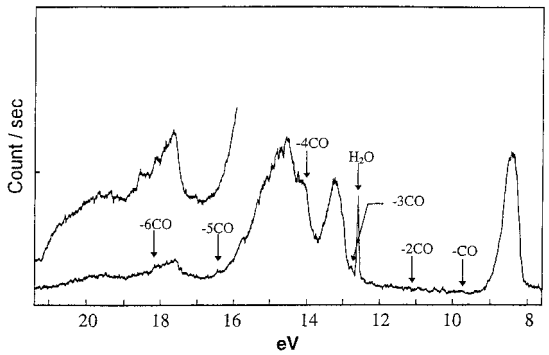

Figure 7. He I photoelectron spectrum of $Mo(CO)_6$ reproduced from (ref 15). The arrows show the onsets of photofragments from $Mo(CO)_6$.

TABLE 2: BDEs of $Mo(CO)_6$ and $Mo(CO)_6^+$

	BDE (eV)			
species	this work	ref 4	ref 3	ref 18
$(CO)_5Mo^+-CO$	1.55 ± 0.02	1.56	1.57	1.34
$(CO)_4Mo^+-CO$	1.38 ± 0.03	1.59	2.1	1.64
$(CO)_3Mo^+-CO$	1.79 ± 0.04	1.68	1.8	1.08
$(CO)_2Mo^+-CO$	1.27 ± 0.04	1.57	1.9	1.54
$(CO)Mo^+-CO$	1.98 ± 0.05	1.66	2.5	1.90
Mo^+-CO	2.01 ± 0.10	1.72	2.6	2.5
$(CO)_2Mo^{2+}-CO$	1.78 ± 0.70		1.7	
$(CO)Mo^{2+}-CO$	3.36 ± 0.80		3.7	
$(CO)Mo^+-C$	2.44 ± 0.50			
Mo^+-C	3.46 ± 0.30		4.7	
$\bar{D}_0(Mo-CO)$	1.84	1.86	2.3	1.87
$\bar{D}_0(Mo^+-CO)$	1.66	1.63	2.1	1.67

await further modeling of the dissociative photoionization kinetics. Recently, high-level theoretical calculations on the BDEs of $(CO)_mMo^+-CO$ have been available. For example, BDE((Mo^+-CO) and BDE($(CO)Mo^+-CO$) have been calculated to be 0.82 and 0.92 eV, respectively, by Barnes et al.[26] While both the theoretical calculation and our experiment show that the two BDEs are quite close, the discrepancy between the calculation and our experiment is significant. This is in fact not surprsing since, as we will show below, the fragmentation process prdoduces an excited state $(Mo^+)^*$ instead of a ground state Mo^+.

Table 2 also includes the BDEs of the doubly charged species and the carbide fragment ions. These BDEs were obtained in a similar way to that described above. For instance, BDE-(Mo^+-C) can be calculated by the following equation:

$$BDE(Mo^+-C) = AP(Mo^+) + BDE(C-O) - AP(MoC^+) \quad (3)$$

where BDE(C−O) is the bond dissociation energy of the free CO (11.158 eV).[25] Of course, all the species near their APs have to be assumed in the ground states in order to estimate the ground state BDE. As will be shown below, however, Mo^+ is actually produced in an excited state near the AP. Therefore, BDE(Mo^+-C) can only be regarded as the energy required to break the Mo^+-C bond with Mo^+ in the excited state.

The average BDEs $\bar{D}_0$(Mo-CO) of $Mo(CO)_6$ and $\bar{D}_0(Mo^+-CO)$ of the $Mo(CO)_6^+$ ion are calculated by the following equations:

$$\bar{D}_0(Mo-CO) = [AP(Mo^+) - IP(Mo)]/6 \quad (4)$$

$$\bar{D}_0(Mo^+-CO) = [AP(Mo^+) - IP(Mo(CO)_6)]/6 \quad (5)$$

where IP(Mo) is the ionization potential of the molybdenum atom (7.099 eV) from the literature.[25] These values are listed in Table 2 as well. It is seen that our data on $\bar{D}_0(Mo-CO)$ and $\bar{D}_0(Mo^+-CO)$ are in good accord with those of Michels et al.[4] and Foffani et al.[14]

In addition, we are able to obtain the second IPs of MoCO (17.44 eV), $Mo(CO)_2$ (16.47 eV), and $Mo(CO)_3$ (15.96 eV) using our AP data through the following relation:

$$IP_{II}(Mo(CO)_n) = AP(Mo^{2+}(CO)_n) - AP(Mo^+(CO)_n) \quad (6)$$

These values are consistently larger than those measured by Winters and co-workers,[3] which are 16.5, 15.2, and 15.4 eV for the second Ips of MoCO, $Mo(CO)_2$, and $Mo(CO)_3$, respectively.

It is interesting to note that the heat of formation of Mo^+ calculated by eq 1 and listed in Table 1 ($\Delta H_f^0{}_{298}(Mo^+) = 358.0$ kcal/mol) is significantly larger than the presently accepted literature value (320.5 kcal/mol).[27] This discrepancy of 37.5 kcal/mol seems larger than could reasonably be attributed to kinetic shifts and reverse activation barriers since in a similar study on $Cr(CO)_6$, we did not observe such discrepancy. We therefore believe that the molybdenum ion is produced in an excited state. Cotton and co-workers proposed that excited states of the metal atom and carbon monoxide might be involved in the bond rupture in the metal carbonyls.[28] Winters and Kiser also suggested that an excited state Mo^+ could be produced by the electron impact ionization/fragmentation.[3] If we assume that

this process might occur in the VUV single-photon ionization fragmentation, represented as

$$Mo(CO)_6 \rightarrow (Mo^+)^* + 6CO + e \quad (7)$$

then the thermochemical relation involving the AP of $(Mo^+)^*$ would be

$$\Delta H_{f\ 298}^{0}((Mo^+)^*) = \Delta H_{f\ 298}^{0}(Mo(CO)_6) + AP((Mo^+)^*) - 6\Delta H_{f\ 298}^{0}(CO) \quad (8)$$

According to Sugar and Musgrove,[29] the lowest excited states of Mo^+ described as ^6D are derived from the configuration $4d^4$-5s. According to various J values, the ^6D term of the Mo^+ ion can split into $^6D_{1/2}$, $^6D_{3/2}$, $^6D_{5/2}$, $^6D_{7/2}$, and $^6D_{9/2}$. Their energy levels are 33.7, 34.4, 35.5, 36.9, and 38.5 kcal/mol above the ground state Mo^+, respectively.[29] As mentioned above, our experimental value (358.0 kcal/mol) is larger by 37.5 kcal/mol than the accepted literature value (320.5 kcal/mol). This value (37.5 kcal/mol)) is close to the energies of the excited states $^6D_{7/2,9/2}$, which is the first excited state of the Mo^+ ion. Therefore, we suggest that the molybdenum ion, formed from the VUV single-photon ionization of $Mo(CO)_6$ followed by dissociation, is left in some excited states of Mo^+, possibly $^6D_{7/2,9/2}$. It should be mentioned that Winters and Kiser attributed the excited state of Mo^+, produced by electron impact ionization/fragmentation, to $d^5\ ^2I_{11/2}$, which lies approximately 66 kcal/mol above the ground state.[3] Clearly, the correctness of the assignment of the excited state of Mo^+ produced by either photoionization or electron impact ionization is largely determined by the accuracy of the AP data.

V. Summary and Conclusions

A detailed study on the PIE curves of 12 ions resulting from the dissociative photoionization of $Mo(CO)_6$ has been carried out for the first time with a synchrotron radiation source in the photon energy range of 8−40 eV. The experimental measurement was accomplished by using a TOF mass spectrometer which uses all the photoelectrons from photoionization for the start pulse, including both threshold and nonthreshold photoelectrons. APs of all the observed ions have been determined and these AP values, in turn, bring about a series of BDE data for the intermediate ions produced by photoionization/fragmentation. The data obtained in this study provide important clues for further theoretical investigations on the metal carbonyl compound.

Acknowledgment. This work is supported by a Grant from the Croucher Foundation (CF95/96.SC02). S.Y. thanks the National Synchrotron Radiation Laboratory in Hefei, China, for an award of using the photochemistry beam line.

References and Notes

(1) *Laser Chemistry of Organometallics*; Chaiken, J., Ed.; ACS Symposium Series 530; American Chemical Society: Washington, DC, 1993.

(2) Wrighton, M. *Chem. Rev*. **1974**, *74*, 401 and references therein.

(3) Winters, R. E.; Kiser, R. W. *Inorg. Chem*. **1965**, *4*, 157.

(4) Michels, G. D.; Flesch, G. D.; Svec, H. J. *Inorg. Chem*. **1980**, *19*, 479.

(5) Das, P. R.; Nishimura, T.; Meisels, G. G. *J. Phys. Chem*. **1985**, *89*, 2808.

(6) Venkataraman, B.; Hou, H. Q.; Zhang, Z. J.; Chen, S. H.; Bandukwalla, G.; Vernon, M. *J. Chem. Phys*. **1990**, *92*, 5338.

(7) Norwood, K.; Ali, A.; Flesch, G. D.; Ng, C. Y. *J. Am. Chem. Soc*. **1990**, *112*, 7502.

(8) Ng, C. Y. *Molecular beam photoionization and photoelectron-photoion coincidence studies of high temperature molecules, transient species, and clusters*. In *Vacuum Ultraviolet Photoionization and Photodissociation of Molecules and Clusters*; Ng, C. Y., Ed.; World Scientific, New Jersey, 1991; pp 101−169.

(9) Qi, F.; Yang, X.; Yang, S. H.; Gao, H.; Sheng, L. S.; Zhang, Y. W.; Yu, S. Q. *J. Chem. Phys.* **1997**, *107*, in press.

(10) (a) Sheng, L. S.; Qi, F.; Tao, L.; Zhang, Y. W.; Yu, S. Q.; Wang, C. K.; Li, W. -K. *Int. J. Mass Spectrom. Ion processes* **1995**, *148*, 179. (b) Qi, F.; Sheng, L. S.; Zhang, Y. W.; Yu, S. Q.; Li, W. -K. *Chem. Phys. Lett*. **1995**, *234*, 450.

(11) Zhang, Y. W.; Sheng, L. S.; Gao, H.; Qi, F. In *Atomic and Molecular Photoionization*; Yagishita, A., Sasaki, T., Eds.; (Universal Academy Press, Inc.: New York, 1996).

(12) For example, see: Traeger, J, C.; Kompe, B. M. *Int. J. Mass Spectrom. Ion Processes* **1990**, *101*, 111.

(13) Tsai, B. P.; Baer, T.; Werner, A. S.; Lin, S. F. *J. Chem. Phys.* **1975**, *79*, 570.

(14) Shiromaru, H.; Achiba, Y.; Kimura, K.; Lee, Y. T. *J. Phys. Chem*. **1987**, *91*, 17.

(15) Turner, D. W. In *Molecular Photoelectron Spectroscopy* Interscience: New York, 1969; Chapter 14.

(16) Johnson, J. B.; Klemperer, W. G. *J. Am. Chem. Soc*. **1977**, *99*, 7132.

(17) Cooper,G.; Sze, K. H.; Brion, C. E. *J. Am. Chem. Soc*. **1990**, *112*, 4121.

(18) Foffani, A.; Pigrataro, S.; Cantone, B.; Grasso, F. *Z. Phys. Chem*. **1965**, *45*, 79.

(19) Cooper, G.; Green, J. C.; Payne, M. P.; Dobson, B. R.; Hillier, I. H. *J. Am. Chem. Soc*. **1987**, *109*, 3836.

(20) Hubbard, J. L.; Lichtenberger, D. L. *J. Am. Chem. Soc*. **1982**, *104*, 2132.

(21) Higginson, B. R.; Lloyd, D. R.; Burroughs, P.; Gibson, D. M.; Orchard, A. F. *J. Chem. Soc., Faraday Trans*. **1973**, *2*, 1659.

(22) (a) Lloyd, D. R.; Schlag, E. W. *Inorg. Chem*. **1969**, *8*, 2544. (b) Vilesov, F. I.; Kurbatov, B. L. *Dokl. Akad. Nauk SSSR* **1961**, *140*, 1364.

(23) Qi, F.; Yang, X.; Yang, S. H.; Liu, F. Y.; Sheng, L. S.; Gao, H.; Zhang, Y. W.; Yu, S. Q. *J. Chem. Phys*. **1997**, *106*, 9474.

(24) Cotton, F. A.; Fischer, A. K.; Wilkinson, G. *J. Am. Chem. Soc*. **1956**, *78*, 5168.

(25) *CRC handbook of Chemistry and Physics*, 72nd ed.; Lide, D. R., Ed.; CRC Press: Boca Raton, FL, 1992.

(26) Barnes, L. A.; Rosi, M; Bauschlicher, C. W. *J. Chem. Phys*. **1990**, *93*, 609.

(27) Lias, S. G.; Bartmess, J. E.; Liebman, J. F.; Holmes, J. L.; Levine, R. D.; Mallard, W. G. *J. Phys. Chem. Ref. Data* **1988**, *17*, (Suppl. 1).

(28) Cotton, F. A.; Fischer, A. K.; Wilkinson, G. *J. Am. Chem. Soc*. **1959**, *81*, 800.

(29) Sugar, J.; Musgrove, A. *J. Phys. Chem. Ref Data* **1988**, *17* (1), 155.